Author Manuscript

Author Manuscript

Author Manuscript

Author Manuscript

HHS Public Access

Author manuscript

J Invest Dermatol. Author manuscript; available in PMC 2022 August 01.

Published in final edited form as:

J Invest Dermatol. 2021 August ; 141(8): 1964–1974. doi:10.1016/j.jid.2020.11.036.

Hair loss caused by gain-of-function mutant TRPV3 is associated with premature differentiation of follicular keratinocytes

Zhongya Song[1,2], **Xi Chen**[2], **Qian Zhao**[1], **Vesna Stanic**[2], **Zhimiao Lin**[1], **Shuxia Yang**[1], **Ting Chen**[3], **Jiang Chen**[2,4,+], **Yong Yang**[1,5,6,+]

[1]Department of Dermatology, Peking University First Hospital, Beijing Key Laboratory of Molecular Diagnosis on Dermatoses and National Clinical Research Center for Skin and Immune Diseases, Beijing, China

[2]Department of Pathology, Stony Brook University, Stony Brook, New York, USA

[3]National Institute of Biological Sciences, Beijing, China

[4]Department of Dermatology, Stony Brook University, Stony Brook, New York, USA

[5]Peking-Tsinghua Center for Life Sciences, Beijing, China

[6]Institute of Dermatology, Chinese Academy of Medical Sciences and Peking Union Medical College, Nanjing, Jiangsu, China

Abstract

Gain-of-function mutations in the *TRPV3* gene can cause Olmsted syndrome characterized by palmoplantar and periorificial keratoderma, itch, and hair loss. The mechanism underlying hair loss remains unclear. Here, we engineered an Olmsted syndrome mouse model by introducing the point mutation G568V to the corresponding *Trpv3* locus in mice. These mice developed fully penetrant hair loss. The hair loss was associated with premature differentiation of follicular keratinocytes characterized by precocious degeneration of trichohyalin and keratins, increased production of deiminated proteins, elevated apoptosis, and attenuation of transcription regulators (*Foxn1*, *Msx2*, *Dlx3*, and *Gata3*) known to regulate hair follicle differentiation. These abnormalities occurred in the medial-proximal region of the inner root sheath and the hair shaft, where *Trpv3* is highly expressed, and correlated with impaired formation of the hair canal and the hair shaft. The mutant *Trpv3* mice also exhibited increased proliferation in the outer root sheath,

Correspondence: Yong Yang, Institute of Dermatology, Chinese Academy of Medical Sciences and Peking Union Medical College, No. 12 Jiangwangmiao Street, Xuanwu District, Nanjing 210042, China. Phone: 86-25-85478067. yyang@pumcderm.cams.cn.
[+]J.C. and Y.Y. contributed equally to this work as senior authors

AUTHOR CONTRIBUTIONS

YY and JC jointly conceptualized and supervised the study. ZS performed most of the experiments. ZS, XC, QZ, VS, ZL, SY, TC, JC and YY are involved in experimental design and data analysis. ZS, JC and YY wrote the manuscript.

CONFLICT OF INTEREST

The authors state no conflict of interest.

Publisher's Disclaimer: This is a PDF file of an unedited manuscript that has been accepted for publication. As a service to our customers we are providing this early version of the manuscript. The manuscript will undergo copyediting, typesetting, and review of the resulting proof before it is published in its final form. Please note that during the production process errors may be discovered which could affect the content, and all legal disclaimers that apply to the journal pertain.

Author Manuscript Author Manuscript Author Manuscript Author Manuscript

accelerated hair cycle, reduction of hair follicle stem cells, and miniaturization of regenerated hair follicles. Findings from this study suggest that precocious maturation of postmitotic follicular keratinocytes drives hair loss in Olmsted syndrome patients.

Keywords

alopecia; keratinocyte; differentiation; deimination; Olmsted syndrome

INTRODUCTION

Transient receptor potential cation channel, subfamily V, member 3 (TRPV3), a nonselective Ca^{2+}-permeable channel (Xu et al., 2002, Luo et al., 2012), is expressed in epidermal and follicular keratinocytes (Peier et al., 2002, Xu et al., 2002, Xu et al., 2006, Huang et al., 2008). Gain-of-function mutations in the *TRPV3* gene can cause hair loss in Olmsted syndrome (OS) (Lin et al., 2012, Duchatelet and Hovnanian, 2015, Zhong et al., 2020). However, the mechanism is unknown.

Formation of the hair follicle and hair shaft requires orchestrated proliferation, differentiation, and death of follicular keratinocytes (Magerl et al., 2001, Vesela and Matalova, 2015, Mesler et al., 2017, Yang et al., 2017). The differentiation of follicular keratinocytes can be arbitrarily divided into early differentiation, where progenitor cells differentiate into respective lineages in the proximal region of hair follicle, and late differentiation, where postmitotic cells of specific lineages terminally differentiate into the hair canal and hair shaft (Sequeira and Nicolas, 2012, Mesler et al., 2017). Early differentiation of hair follicles is controlled by signaling pathways, including bone morphogenic protein and hedgehog (Kobielak et al., 2003, Abe and Tanaka, 2017) in the proximal hair follicles, whereas late differentiation is controlled by transcription regulators, such as FOXN1, MSX2, DLX3 and GATA3 (Mecklenburg et al., 2001, Kaufman et al., 2003, Ma et al., 2003, Hwang et al., 2008), proceeding to the formation of the hair canal or the hair shaft.

During late differentiation, cellular contents of follicular keratinocytes, including trichohyalin (TCHH) and keratins, undergo posttranslational modifications. One of these processes is deimination (also called citrullination), through which arginine residues in target proteins are converted to citrullines by peptidyl arginine deiminases (Tarcsa et al., 1997, Candi et al., 2005). In the hair follicle, TCHH is a principle substrate of deimination (Candi et al., 2005, Nachat et al., 2005), whereas peptidyl arginine deiminase, type III (PADI3) is the key deiminase (Nachat et al., 2005, Mechin et al., 2020). Deiminated TCHH and keratins become soluble and are readily cross-linked by transglutaminases to form rigid structures such as the hair canal and the hair shaft (Steinert et al., 2003, Candi et al., 2005). Mutations in *PADI3*, transglutaminase 3 (*TGM3*), can lead to uncombable hair syndrome or central centrifugal cicatricial alopecia, underscoring the important roles of protein modifications in hair formation (Basmanav et al., 2016, Malki et al., 2019). Pertinent to this study, the enzymatic activities of peptidyl arginine deiminases and transglutaminases are Ca^{2+} dependent (Candi et al., 2005, Mechin et al., 2020), suggesting that tightly

Author Manuscript Author Manuscript Author Manuscript Author Manuscript

regulated intracellular Ca^{2+} levels are essential for differentiated follicular keratinocytes to form the hair canal and the hair shaft.

In this study, we engineered a *Trpv3* knock-in mouse model to mimic hair loss in patients and found that the disease-causing mutant *Trpv3* can induce premature differentiation of the inner root sheath (IRS) and hair shaft, concomitant with elevated levels of deiminated proteins and attenuation of transcription factors that regulate the differentiation of the hair follicle. Premature differentiation compromised the hair canal and hair shaft, preventing the hair shaft from emerging from the skin. Moreover, perpetuated structural abnormalities in the hair follicles led to the reduction of hair follicle stem cells, leading to impaired hair follicle regeneration. Findings from this study demonstrate a role of TRPV3 in promoting hair follicle differentiation and suggest that premature differentiation caused by gain-of-function mutant TRPV3 is primarily responsible for hair loss in OS patients.

RESULTS

TRPV3 is predominantly expressed in medial-proximal IRS and hair shaft

To gain insight into the potential functions of TRPV3 in the hair follicle, we examined *Trpv3* expression, in conjunction with *Gata3* (expressed in IRS) and *Tchh* (expressed in IRS and medulla), by *in situ* hybridization, and found that *Trpv3* transcripts were predominantly expressed in the medial-proximal IRS and hair shaft in postnatal day (P) 12 mice (Figure 1a–c), consistent with that of *TRPV3* in human hair follicles (Figure 1d, Supplementary Figure S1c). The expression of *Trpv3* first appears in the differentiating cone of hair follicles during early morphogenesis, peaks at growing phase, and becomes undetectable in telogen hair follicles (Supplementary Figure S1a). *Trpv3* is expressed at relatively low level in differentiated epidermal keratinocytes, distal companion layer of the hair follicles, and sebocytes (Figure 1a and Supplementary Figure S1a).

To confirm TRPV3 expression pattern at the protein level, we performed immunofluorescence staining with commercial antibodies, but were unable to obtain consistent results. Thus, we engineered a *Trpv3* reporter mouse model, in which FLAG is fused to the C-terminus of TRPV3 (Supplementary Figure S2). Immunofluorescent labeling of FLAG in conjunction with TCHH (by the AE15 antibody) or KRT75 (expressed in companion layer) demonstrated that TRPV3-FLAG is indeed expressed in medial-proximal IRS and hair shaft (Figure 1e), consistent with the *in situ* hybridization findings. The expression pattern suggests that TRPV3 may be involved in the formation or function of the IRS and hair shaft.

A *Trpv3 (G568V)* knock-in mouse model mimicked hair loss of OS

To determine the nature of the c.1703G/T (p.G568V) mutation (Nagai et al., 2017, Choi et al., 2018), we carried out electrophysiology experiments after transfecting HEK293T cells with wild type or TRPV3-G568V expression plasmids. Measurements on TRPV3-G568V transfected cells exhibited profiles typical for a gain-of-function mutant TRPV3 (Supplementary Fig. S3).

Author Manuscript Author Manuscript Author Manuscript Author Manuscript

Trpv3 is a highly conserved gene, and the peptide sequences of human and mouse TRPV3 share 93% similarity (Supplementary Figure S4a). To investigate the mechanism underlying hair loss in OS patients, we engineered a *Trpv3* knock-in mouse model by introducing G568V to the corresponding locus in mice through embryonic stem cell targeting (Supplementary Figure S4b). Successful construction of this mutant *Trpv3* mouse model was confirmed by Sanger sequencing of genomic DNA, qRT-PCR (quantitative real-time reverse transcriptase-PCR), and western blotting (Supplementary Figure S4c–e).

Heterozygous and homozygous *Trpv3* knock-in mice ($Trpv3^{+/G568V}$ and $Trpv3^{G568V/G568V}$, respectively) were born at expected Mendelian ratio and were phenotypically indistinguishable from control littermates ($Trpv3^{+/+}$) before P5 (Figure 2a). By P12, $Trpv3^{+/G568V}$ pups started to lose hair around the neck, whereas $Trpv3^{G568V/G568V}$ littermates exhibited marked hair loss (Figure 2a). By P21, both $Trpv3^{+/G568V}$ and $Trpv3^{G568V/G568V}$ mice progressed to extensive hair loss (Figure 2a). No gender difference was noticed. Considering that the *Trpv3* knock-in mouse models mimicked the hair loss in OS, these mouse models may be used to understand the mechanisms underlying hair loss in OS patients.

Hair follicle and hair shaft in *Trpv3* knock-in mice developed structural abnormalities

Hematoxylin and eosin (H&E) staining demonstrated that hair follicles in *Trpv3* knock-in mice exhibited normal histology at P5 prior to the development of gross phenotypes (Figure 2b). However, at P12, the distal portion of hair follicles in *Trpv3* knock-in mice appeared bent and curled, and hair shafts were unable to penetrate and emerge from the skin (Figure 2b). At P21, the hair follicles in $Trpv3^{+/+}$ mice regressed to telogen, whereas hair follicles in *Trpv3* knock-in mice developed into keratinized cysts (Figure 2b).

Scanning electron microscopy demonstrated irregularities and reduced intercalation of hair shaft cuticles in $Trpv3^{+/G568V}$ mice at P12. In $Trpv3^{G568V/G568V}$ mice, few hair shafts emerged from the skin, but they appeared fractured and devoid of cuticles (Supplementary Figure S5a).

At P5, the *Trpv3* transcripts in $Trpv3^{G568V/G568V}$ mice exhibited a normal expression pattern (Supplementary Figure S5b) before phenotypes appeared. At P12, the *Trpv3* transcripts became restricted to the proximal region of hair follicles (Supplementary Figure S5c), coinciding with the development of gross and histological phenotypes. Thus, we focused on the proximal hair follicles at approximately 500 μm under the skin surface (as illustrated in Figure 4c). Transmission electron microscopy demonstrated that hair follicles in $Trpv3^{+/+}$ mice exhibited distinctive concentric layers, namely the outer root sheath (ORS), companion layer, IRS (Henle's layer, Huxley's layer, and cuticle) and hair shaft (cuticle, cortex, medulla), and TCHH granules and keratin bundles were readily visible (Figure 2c). In hair follicles of $Trpv3^{+/G568V}$ mice, all layers are recognizable, but the ORS and IRS were thickened, cells in the Huxley's layer appeared amorphous with no TCHH granules but apoptotic nuclei, whereas cells in the hair cortex lacked characteristic keratin bundles (Figure 2c). Strikingly, most hair follicles in $Trpv3^{+/G568V}$ mice developed an electron-light gap demarcated by the hair shaft cuticle and IRS cuticle (Figure 2c–d). This gap is otherwise observable in normal hair follicles at 200 μm underneath the epidermis when mature hair

Author Manuscript Author Manuscript Author Manuscript Author Manuscript

shaft detaches from the IRS (Supplementary Figure S5d) (Alibardi, 2004, Harland and Plowman, 2018). These ultrastructural abnormalities in the proximal hair follicles of *Trpv3* knock-in mice indicated that expression of the mutant *Trpv3* induced precocious maturation of the hair follicles.

Impaired hair follicle differentiation in *Trpv3* knock-in mice

Follicular keratinocyte differentiation was evaluated by the expression of keratins. Immunofluorescence demonstrated that KRT71 in IRS, KRT82 in hair shaft cuticle, and hair cortex keratins labeled by the AE13 antibody, were markedly diminished in the medial region of the hair follicles in P12 $Trpv3^{G568V/G568V}$ mice (Figure 3a). In contrast, KRT75, a marker for the proximal companion layer, where *Trpv3* is undetectable, was unperturbed (Figure 3a). These findings were further confirmed by western blotting (Figure 3b and Supplementary Figure S6). As prior morphological analyses (Figure 2b–c) demonstrated the existence of respective layers in $Trpv3^{G568V/G568V}$ mice, reduced expression of these keratin markers suggests that the mutant *Trpv3* did not affect the formation but the late differentiation of follicular keratinocytes in which it is expressed.

Differentiation markers of the epidermis, KRT1 and Loricrin (LOR), were also significantly expanded in P12 $Trpv3^{G568V/G568V}$ mice (Supplementary Figure S7), further substantiating the role of the mutant *Trpv3* in keratinocyte differentiation.

Expression of the mutant *Trpv3* led to increased protein deimination

To further evaluate hair follicle differentiation, we examined the key substrates and enzymes involved in protein deimination (as illustrated in Figure 4a). The native or unprocessed form of TCHH, a principle substrate of protein deimination in the hair follicle, detectable by immunofluorescence with the AE15 antibody (O'Guin et al., 1992), was normally expressed in the medial-proximal region of the IRS and the medulla of hair follicles (Figure 4b). However, in $Trpv3^{G568V/G568V}$ mice, TCHH was essentially absent from the medial region of the hair follicles (Figure 4b), indicating a possibility of being further processed posttranslationally, hence becoming undetectable.

Deiminated proteins, as demonstrated by immunohistochemistry, were restricted to the distal-medial portion of control hair follicles (Figure 4c). Quantification demonstrated that in control mice deiminated proteins are detectable at approximately 287.4 ± 24.1 μm distally from the Auber's line or occupying approximately 41.2 ± 1.9 % of the distal region of the nonpermanent portion of a mature hair follicle (Figure 4c). In $Trpv3^{G568V/G568V}$ mice, deiminated proteins substantially extended to the proximal portion of anagen hair follicles such that they became detectable at approximately 92.3 ± 6.7 μm distally from the Auber's line or occupying 64.0 ± 3.8% of distal portion of the nonpermanent part of mature hair follicles (Figure 4d). The concomitant reduction of native TCHH and elevated level of deiminated proteins in the medial-proximal portion of mature hair follicles suggest that TCHH was expressed but prematurely deiminated in the IRS and medulla of *Trpv3* knock-in mice. Consistently, *in situ* hybridization demonstrated that the levels of *Padi3* and *Tgm3* were markedly reduced in the medial-proximal region of hair follicle in $Trpv3^{G568V/G568V}$ mice (Figure 4e), where protein deimination had already occurred (as shown in Figure 4c).

Author Manuscript Author Manuscript Author Manuscript Author Manuscript

These findings suggest that the TRPV3-G568V promotes protein deimination in the hair follicles.

Apoptosis is a hallmark of late differentiation of the hair follicle. TUNEL staining in *Trpv3*$^{G568V/G568V}$ mice demonstrated markedly increased apoptotic cells in the medial-distal region of IRS, whereas cell in the medial-proximal region became apoptotic prematurely (Figure 4f–g and Supplementary Figure S8), suggesting that increased cell death was associated with accelerated differentiation.

Transcriptional regulators of hair follicle differentiation were suppressed in *Trpv3* knock-in mice

The premature but orchestrated hair follicle differentiation indicates that the mutant TRPV3 might have impaired the regulation of hair follicle differentiation at the transcriptional level. *In situ* hybridization demonstrated comparable expression patterns of *Axin2* and *Ptch1* of the Wnt and hedgehog signaling pathways, respectively (Figure 5a), suggesting that early differentiation of the hair follicles in *Trpv3*$^{G568V/G568V}$ mice was normal. In contrast, *Foxn1*, *Msx2*, *Dlx3*, and *Gata3*, which were implicated in later stages of hair follicle differentiation, were markedly attenuated in P12 *Trpv3*$^{G568V/G568V}$ mice (Figure 5b). At P5, expression of these transcription factors were comparable between control and *Trpv3*$^{G568V/G568V}$ littermates, consistent with the absence of obvious skin phenotypes (Supplementary Figure S9). Because that the expression patterns of these signaling molecules correlate with that of *Trpv3* and that the hair follicles phenotypes observed in loss-of-function mutant mice models of *Foxn1*, *Msx2*, *Dlx3*,and *Gata3* (Mecklenburg et al., 2001, Kaufman et al., 2003, Ma et al., 2003, Hwang et al., 2008) share striking similarities with those in the mutant *Trpv3* mice, it is conceivable that TRPV3 and these transcriptional regulators operate in the same regulatory network to safeguard late differentiation of the hair follicles.

Progressive hair loss and abnormal hair cycle in *Trpv3* knock-in mice

Despite that *Trpv3* knock-in mice exhibited remarkable hair loss during postnatal morphogenesis, hair shafts could emerge during subsequent anagens (Figure 6a and Supplementary Figure S10), albeit telogen hair follicles became atypical and the hair cycle became abnormal. Moreover, alkaline phosphatase staining demonstrated that the hair follicle density in P249 *Trpv3* knock-in mice were significantly reduced and the hair follicles were no longer polarized in the anterior-posterior orientation (Figure 6b–d), likely caused by severely compromised hair canal and thickened epidermis. Moreover, there is a decline of histologically normal hair follicles in *Trpv3* knock-in mice (Figure 6e and Supplementary Figure S10). These findings suggest that the expression of the mutant *Trpv3* impaired hair follicle regeneration.

BrdU labeling revealed slightly reduced proliferating cells in the hair matrix, but significantly increased proliferating cells in the distal ORS and infundibulum of *Trpv3*$^{G568V/G568V}$ mice (Figure 6f and 6g). Immunofluorescence of CD34 and NFATC1 demonstrated that hair follicle stem cells were significantly reduced in *Trpv3*$^{G568V/G568V}$ mice (Figure 6h–j). These data suggest that perpetuated expression of the mutant *Trpv3* in

Author Manuscript Author Manuscript Author Manuscript Author Manuscript

the IRS and medulla of hair follicles may lead to hyperactivation and gradual exhaustion of hair follicle stem cells, attributing to progressive hair loss.

DISCUSSION

The utilization of loss-of-function mouse models or *ex vivo* models were valuable in understanding the biological functions of TRPV3 (Cheng et al., 2010, Borbiro et al., 2011). The previously identified positive feedback between EGFR signaling pathway and TRPV3 is instrumental in guiding the use of erlotinib, an EGFR inhibitor, to improve palmoplantar keratoderma in OS patients (Greco et al., 2020, Zhang et al., 2020). However, this mechanism may not be used to explain hair loss in OS patients as erlotinib treatment was associated with exacerbation of hair loss (Greco et al., 2020, Zhang et al., 2020). The *Trpv3* knock-in mouse models reported herein recapitulated hair loss of OS both genetically and phenotypically, suggesting that the pathogenesis underlying hair loss in these mouse models is likely parallel with that of OS patients. Moreover, the DS-*Nh* mice (Asakawa et al., 2006, Imura et al., 2007), which harbor a dominant mutant TRPV3 (G573S), exhibited hair phenotypes that were, to a large extent, similar to those observed in the *Trpv3* knock-in mouse models described herein, confirming the detrimental effect of dominant mutant *Trpv3* on hair formation.

The hair follicle phenotypes in *Trpv3* knock-in mice temporally and spatially correlated with the expression profile of *Trpv3*, and severely affected differentiation events of keratinocytes in the IRS and hair shaft compartments. Abnormalities observed in other follicular compartments where *Trpv3* expression is low or undetectable, including increased proliferation in distal hair follicles, reduction of stem cells, and accelerated hair cycle, were likely secondary but contributed collectively to the phenotypic outcome.

The premature differentiation developed coordinately in the IRS and in the hair shaft, and is accompanied by increased cell death, suggesting that *Trpv3* acts as an upstream regulator of late differentiation. It is plausible that the gain-of-function mutant TRPV3 activates Ca^{2+} influx (Lin et al., 2012), thereby, increases intracellular concentration of Ca^{2+}, which could trigger keratinocyte differentiation and catalyze PADI3 and TGM3 enzymatic activities required for differentiating keratinocytes. The marked apoptosis in the hair follicles of *Trpv3* knock-in mice may be attributable to increased differentiation and to increased PADI3 activity, which can directly induce apoptosis (Lange et al., 2011, Jamali et al., 2016). Considering that the expression pattern of *Trpv3* closely resembles those of *Foxn1*, *Msx2*, *Dlx3* and *Gata3*, and that phenotypes in *Trpv3* knock-in mice resemble those in loss-of-function mutant mouse models of these transcription regulators (Mecklenburg et al., 2001, Kaufman et al., 2003, Ma et al., 2003, Hwang et al., 2008) that play critical roles in regulating follicular keratinocyte differentiation, it is also plausible that the gain-of-function mutant TRPV3 promoted keratinocyte differentiation by downregulating these transcription regulators.

In addition to this study, mutations in genes implicated in late stage keratinocyte differentiation have been associated with a number of hair disorders, including uncombable hair syndrome (Basmanav et al., 2016) and central centrifugal cicatricial alopecia (Malki

Author Manuscript Author Manuscript Author Manuscript Author Manuscript

et al., 2019). These findings demonstrate that impairment in protein modifications in differentiated follicular keratinocytes is an important contributor to hair abnormalities. Understanding the interplay of factors in regulating late differentiation of follicular keratinocytes will shed light on how hair follicles can produce hair shafts with divergent appearances and how impaired differentiation can lead to various forms of hair disorders.

MATERIALS AND METHODS

Animals

Trpv3-Flag mice were generated through CRISPR/Cas9 genome editing by Shanghai Biomodel Organism Science and Technology Development Co.,Ltd (Shanghai, China). *Trpv3* knock-in mice (*Trpv3*$^{+/G568V}$) were generated through ES cell targeting by Cyagen Biosciences Inc (Suzhou, China). Detailed information can be found in Supplementary Materials and Methods. Wild-type (*Trpv3*$^{+/+}$) littermates were used as controls. All animal experiments were approved by the Institutional Animal Care and Use Committees of Stony Brook University (#1301865) and Peking University First Hospital (#201739).

Ethical approval for human specimens

Human specimens were obtained after written informed consent and were approved by institutional review board of the Institute of Dermatology of the Chinese Academy of Medical Sciences (2019-KY-001).

RNA isolation and qRT-PCR

Total RNA was isolated from dorsal whole skin of mice. qRT-PCR analyses were performed as described previously (Dai et al., 2013). More details can be found in the Supplementary Materials and Methods.

Histology, immunofluorescence labeling, and electron microscopy

Skin samples were collected and fixed immediately in 10% neutral buffered formalin overnight, embedded in paraffin, sectioned for 6 μm and processed for histology. Details of immunofluorescence labeling and scanning and transmission electron microscopy protocols can be found in the Supplementary Materials and Methods.

Detection of deiminated or citrullinated proteins

Deiminated proteins were detected by using an anti-citrulline detection kit (17–347B-1, Millipore). Briefly, paraffin-embedded tissue sections were deparaffinized, rehydrated, and incubated in modification medium (0.0125% $FeCl_3$, 0.125 M H_2SO_4, 0.1 M H_3PO_4, 0.25% 2,3-butanedione monoxime, 0.125% antipyrine and 0.25 M acetic acid) at 37 °C for 3 hours. Sections were subsequently blocked in 5% nonfat dry milk in PBS for 1 hour at room temperature, incubated with human anti-modified citrulline antibody (1 ug/ml) for 1 hour at 37°C, and incubated with HRP-conjugated goat anti-human antibody (1:500) for 1 hour at room temperature. Sections were then incubated with ImmPACT™ AMEC Red Peroxidase Substrate (SK-4285, Vector Laboratory, Burlingame, CA) for 30 minutes at room

Author Manuscript Author Manuscript Author Manuscript Author Manuscript

temperature and mounted with VectaMount® AQ Aqueous Mounting Medium (H-5501, Vector Laboratory, Burlingame, CA).

BrdU labeling and TUNEL staining

To detect proliferating cells, 10 μl BrdU (000103, Life Technologies, Carlsbad, CA) per gram of body weight was injected to mice intraperitoneally 2 hours before euthanization and tissue collection. BrdU-positive cells were detected by immunofluorescence labeling. To detect cell apoptosis, DeadEnd Fluorometric TUNEL system (G3250, Promega, Fitchburg, WI) was used per the manufacturer's instruction.

In situ hybridization

Formalin-fixed and paraffin-embedded tissue sections were used for *in situ* hybridization with the RNAScope system (Advanced Cell Diagnostic, Hayward, CA) per the manufacturer's instruction and as previously described (Wang et al., 2012, Chen et al., 2015).

Alkaline phosphatase staining

Alkaline phosphatase staining was performed as previously described (Chen et al., 2015). Briefly, fresh skin was fixed in 4% paraformaldehyde for 10 minutes, and soaked in B3 buffer (0.1 M Tris, pH 9.5, 0.1 M NaCl, and 0.05 M MgCl2) for 10 minutes, and incubated in NBT/BCIP working solution (72091, MilliporeSigma, St. Louis, MO) for 20 minutes. Stained skins were imaged on a Zeiss (Thornwood, NY) Stemi 2000-C dissecting microscope fitted with an Infinity 2 camera.

Western blotting

Protein was extracted from whole dorsal skin of mice in cold RIPA lysis buffer supplemented with proteinase inhibitors. More details can be found in the Supplementary Materials and Methods.

Statistical analyses

Quantifications are presented as mean ± standard deviation unless otherwise stated. Two-tailed Student's unpaired *t* test was used unless otherwise stated. One-way ANOVA was conducted using GraphPad software (GraphPad Software, Inc., San Diego, CA). $P < 0.05$ was considered statistically significant.

Supplementary Material

Refer to Web version on PubMed Central for supplementary material.

ACKNOWLEDGMENTS

We would like to thank Linghan Hu (Peking University) for electrophysiological experiments; Dr. Dennis R. Roop (University of Colorado Denver Anschutz Medical Campus) and Dr. Tung-Tien Sun (New York University) for antibodies; Susan Van Horn (Central Microscopy Imaging Center, Stony Brook University) and Ya-Chen Chuang and Chung-Chueh Chang (Advanced Energy Research and Technology Center, Stony Brook University) for assistance with electron microscopy. This study was supported by the National Natural Science Foundation of China (Grant No. 81673044 and 81425020 to YY) and the Non-profit Central Research Institute Fund of Chinese

Author Manuscript Author Manuscript Author Manuscript Author Manuscript

Academy of Medical Sciences (Grant No. 2018RC31004 to YY), China Scholarship Council (201706010325 to ZS) and research grants from NIH/NIAMS (AR061485 and AR071573 to JC).

DATA AVAILABILITY STATEMENT

No datasets were generated or analyzed in this study.

Abbreviations:

TRPV3	transient receptor potential cation channel, subfamily V, member 3
OS	Olmsted syndrome
PADI3	peptidyl arginine deiminase, type III
TGM3	transglutaminase 3
TCHH	trichohyalin
IRS	inner root sheath
ORS	outer root sheath
P	postnatal day

REFERENCE

Abe Y, Tanaka N. Roles of the Hedgehog Signaling Pathway in Epidermal and Hair Follicle Development, Homeostasis, and Cancer. J Dev Biol 2017;5(4).

Alibardi L Fine structure and immunocytochemistry of monotreme hairs, with emphasis on the inner root sheath and trichohyalin-based cornification during hair evolution. J Morphol 2004;261(3):345–63. [PubMed: 15281062]

Asakawa M, Yoshioka T, Matsutani T, Hikita I, Suzuki M, Oshima I, et al. Association of a mutation in TRPV3 with defective hair growth in rodents. J Invest Dermatol 2006;126(12):2664–72. [PubMed: 16858425]

Borbiro I, Lisztes E, Toth BI, Czifra G, Olah A, Szollosi AG, et al. Activation of transient receptor potential vanilloid-3 inhibits human hair growth. J Invest Dermatol 2011;131(8):1605–14. [PubMed: 21593771]

Candi E, Schmidt R, Melino G. The cornified envelope: a model of cell death in the skin. Nat Rev Mol Cell Biol 2005;6(4):328–40. [PubMed: 15803139]

Chen J, Laclef C, Moncayo A, Snedecor ER, Yang N, Li L, et al. The ciliopathy gene Rpgrip1l is essential for hair follicle development. J Invest Dermatol 2015;135(3):701–9. [PubMed: 25398052]

Cheng X, Jin J, Hu L, Shen D, Dong XP, Samie MA, et al. TRP channel regulates EGFR signaling in hair morphogenesis and skin barrier formation. Cell 2010;141(2):331–43. [PubMed: 20403327]

Choi JY, Kim SE, Lee SE, Kim SC. Olmsted Syndrome Caused by a Heterozygous p.Gly568Val Missense Mutation in TRPV3 Gene. Yonsei Med J 2018;59(2):341–4. [PubMed: 29436206]

Dai D, Li L, Huebner A, Zeng H, Guevara E, Claypool DJ, et al. Planar cell polarity effector gene Intu regulates cell fate-specific differentiation of keratinocytes through the primary cilia. Cell Death Differ 2013;20(1):130–8. [PubMed: 22935613]

Duchatelet S, Hovnanian A. Olmsted syndrome: clinical, molecular and therapeutic aspects. Orphanet J Rare Dis 2015;10:33. [PubMed: 25886873]

Greco C, Leclerc-Mercier S, Chaumon S, Doz F, Hadj-Rabia S, Molina T, et al. Use of Epidermal Growth Factor Receptor Inhibitor Erlotinib to Treat Palmoplantar Keratoderma in Patients With Olmsted Syndrome Caused by TRPV3 Mutations. JAMA Dermatol 2020;156(2).

Author Manuscript Author Manuscript Author Manuscript Author Manuscript

Harland DP, Plowman JE. The Hair Fibre: Proteins, Structure and Development. Adv Exp Med Biol 2018;1054:109–54. [PubMed: 29797272]

Huang SM, Lee H, Chung MK, Park U, Yu YY, Bradshaw HB, et al. Overexpressed transient receptor potential vanilloid 3 ion channels in skin keratinocytes modulate pain sensitivity via prostaglandin E2. J Neurosci 2008;28(51):13727–37. [PubMed: 19091963]

Hwang J, Mehrani T, Millar SE, Morasso MI. Dlx3 is a crucial regulator of hair follicle differentiation and cycling. Development 2008;135(18):3149–59. [PubMed: 18684741]

Imura K, Yoshioka T, Hikita I, Tsukahara K, Hirasawa T, Higashino K, et al. Influence of TRPV3 mutation on hair growth cycle in mice. Biochem Biophys Res Commun 2007;363(3):479–83. [PubMed: 17888882]

Jamali H, Khan HA, Tjin CC, Ellman JA. Cellular Activity of New Small Molecule Protein Arginine Deiminase 3 (PAD3) Inhibitors. ACS Med Chem Lett 2016;7(9):847–51. [PubMed: 27660689]

Kaufman CK, Zhou P, Pasolli HA, Rendl M, Bolotin D, Lim KC, et al. GATA-3: an unexpected regulator of cell lineage determination in skin. Genes Dev 2003;17(17):2108–22. [PubMed: 12923059]

Kobielak K, Pasolli HA, Alonso L, Polak L, Fuchs E. Defining BMP functions in the hair follicle by conditional ablation of BMP receptor IA. J Cell Biol 2003;163(3):609–23. [PubMed: 14610062]

Lange S, Gogel S, Leung KY, Vernay B, Nicholas AP, Causey CP, et al. Protein deiminases: new players in the developmentally regulated loss of neural regenerative ability. Dev Biol 2011;355(2):205–14. [PubMed: 21539830]

Lin Z, Chen Q, Lee M, Cao X, Zhang J, Ma D, et al. Exome sequencing reveals mutations in TRPV3 as a cause of Olmsted syndrome. Am J Hum Genet 2012;90(3):558–64. [PubMed: 22405088]

Luo J, Stewart R, Berdeaux R, Hu H. Tonic inhibition of TRPV3 by Mg2+ in mouse epidermal keratinocytes. J Invest Dermatol 2012;132(9):2158–65. [PubMed: 22622423]

Ma L, Liu J, Wu T, Plikus M, Jiang TX, Bi Q, et al. 'Cyclic alopecia' in Msx2 mutants: defects in hair cycling and hair shaft differentiation. Development 2003;130(2):379–89. [PubMed: 12466204]

Magerl M, Tobin DJ, Muller-Rover S, Hagen E, Lindner G, McKay IA, et al. Patterns of proliferation and apoptosis during murine hair follicle morphogenesis. J Invest Dermatol 2001;116(6):947–55. [PubMed: 11407986]

Malki L, Sarig O, Romano MT, Mechin MC, Peled A, Pavlovsky M, et al. Variant PADI3 in Central Centrifugal Cicatricial Alopecia. N Engl J Med 2019;380(9):833–41. [PubMed: 30763140]

Mechin MC, Takahara H, Simon M. Deimination and Peptidylarginine Deiminases in Skin Physiology and Diseases. Int J Mol Sci 2020;21(2).

Mecklenburg L, Nakamura M, Sundberg JP, Paus R. The nude mouse skin phenotype: the role of Foxn1 in hair follicle development and cycling. Exp Mol Pathol 2001;71(2):171–8. [PubMed: 11599924]

Mesler AL, Veniaminova NA, Lull MV, Wong SY. Hair Follicle Terminal Differentiation Is Orchestrated by Distinct Early and Late Matrix Progenitors. Cell Rep 2017;19(4):809–21. [PubMed: 28445731]

Nachat R, Mechin MC, Charveron M, Serre G, Constans J, Simon M. Peptidylarginine deiminase isoforms are differentially expressed in the anagen hair follicles and other human skin appendages. J Invest Dermatol 2005;125(1):34–41. [PubMed: 15982300]

Nagai H, Takaoka Y, Sugano A, Nakamachi Y, Kawano S, Nishigori C. Identification of a heterozygous p.Gly568Val missense mutation in the TRPV3 gene in a Japanese patient with Olmsted syndrome: In silico analysis of TRPV3. J Dermatol 2017;44(9):1059–62. [PubMed: 28391651]

O'Guin WM, Sun TT, Manabe M. Interaction of trichohyalin with intermediate filaments: three immunologically defined stages of trichohyalin maturation. J Invest Dermatol 1992;98(1):24–32. [PubMed: 1728637]

Peier AM, Reeve AJ, Andersson DA, Moqrich A, Earley TJ, Hergarden AC, et al. A heat-sensitive TRP channel expressed in keratinocytes. Science 2002;296(5575):2046–9. [PubMed: 12016205]

Sequeira I, Nicolas JF. Redefining the structure of the hair follicle by 3D clonal analysis. Development 2012;139(20):3741–51. [PubMed: 22991440]

Author Manuscript Author Manuscript Author Manuscript Author Manuscript

Steinert PM, Parry DA, Marekov LN. Trichohyalin mechanically strengthens the hair follicle: multiple cross-bridging roles in the inner root shealth. J Biol Chem 2003;278(42):41409–19. [PubMed: 12853460]

Tarcsa E, Marekov LN, Andreoli J, Idler WW, Candi E, Chung SI, et al. The fate of trichohyalin. Sequential post-translational modifications by peptidyl-arginine deiminase and transglutaminases. J Biol Chem 1997;272(44):27893–901. [PubMed: 9346937]

Ü Basmanav FB, Cau L, Tafazzoli A, Mechin MC, Wolf S, Romano MT, et al. Mutations in Three Genes Encoding Proteins Involved in Hair Shaft Formation Cause Uncombable Hair Syndrome. Am J Hum Genet 2016;99(6):1292–304. [PubMed: 27866708]

Vesela B, Matalova E. Detection of Bim and Puma in mouse hair follicles using immunofluorescence and TUNEL assay double staining. Biotech Histochem 2015;90(8):587–93. [PubMed: 26179069]

Wang F, Flanagan J, Su N, Wang LC, Bui S, Nielson A, et al. RNAscope: a novel in situ RNA analysis platform for formalin-fixed, paraffin-embedded tissues. J Mol Diagn 2012;14(1):22–9. [PubMed: 22166544]

Xu H, Delling M, Jun JC, Clapham DE. Oregano, thyme and clove-derived flavors and skin sensitizers activate specific TRP channels. Nat Neurosci 2006;9(5):628–35. [PubMed: 16617338]

Xu H, Ramsey IS, Kotecha SA, Moran MM, Chong JA, Lawson D, et al. TRPV3 is a calcium-permeable temperature-sensitive cation channel. Nature 2002;418(6894):181–6. [PubMed: 12077604]

Yang H, Adam RC, Ge Y, Hua ZL, Fuchs E. Epithelial-Mesenchymal Micro-niches Govern Stem Cell Lineage Choices. Cell 2017;169(3):483–96 e13. [PubMed: 28413068]

Zhang A, Duchatelet S, Lakdawala N, Tower RL, Diamond C, Marathe K, et al. Targeted Inhibition of the Epidermal Growth Factor Receptor and Mammalian Target of Rapamycin Signaling Pathways in Olmsted Syndrome. JAMA Dermatol 2020;156(2).

Zhong W, Hu L, Cao X, Zhao J, Zhang X, Lee M, et al. Genotype-Phenotype Correlation of TRPV3-Related Olmsted Syndrome. J Invest Dermatol 2020.

Author Manuscript Author Manuscript Author Manuscript Author Manuscript

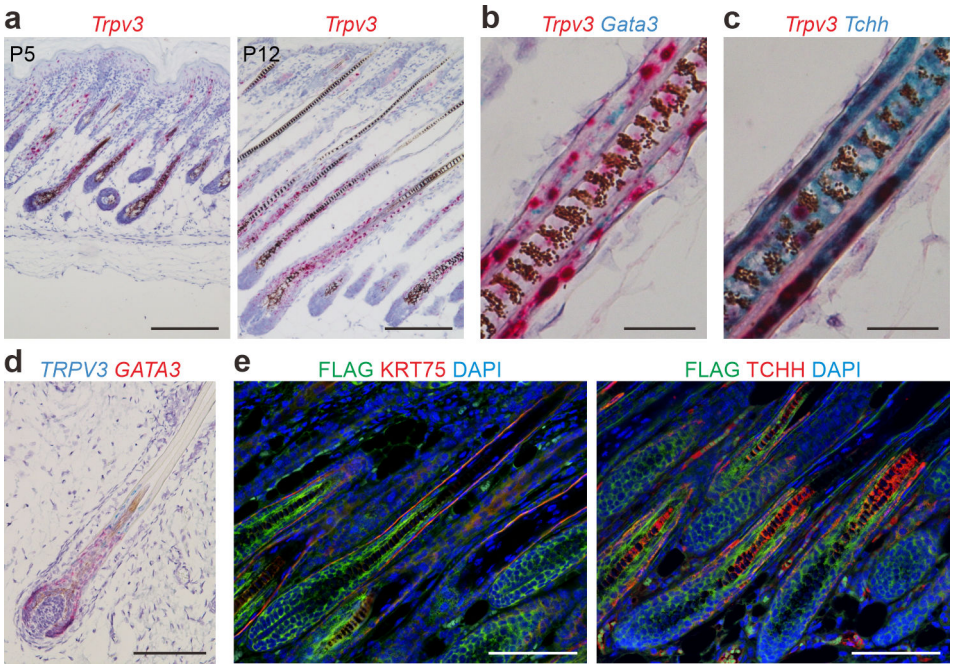

Figure 1. *Trpv3* expression pattern in hair follicles.

(**a**) *In situ* hybridization of *Trpv3* (pink) in dorsal skins of postnatal (P) 5 and P12 mice. (**b - c**) Duplex *in situ* hybridization of *Trpv3* (pink) and *Gata3* (cyan) in (**b**) and *Trpv3* (pink) and *Tchh* (cyan) in (**c**) in dorsal skins of P12 mice. (**d**) *In situ* hybridization of *TRPV3* (cyan) and *GATA3* (pink) in a human fetus scalp hair follicle. (**e**) Immunofluorescence labeling of FLAG and KRT75 or TCHH (with the AE15 antibody) in dorsal skins of P8 *Trpv3-Flag* knock-in mice. Nuclei were stained with hematoxylin (blue, **a - d**) or labeled with DAPI (blue, **e**). Scale bar = 200 μm (**a**), 25 μm (**b - c**), 100 μm (**d - e**).

Author Manuscript Author Manuscript Author Manuscript Author Manuscript

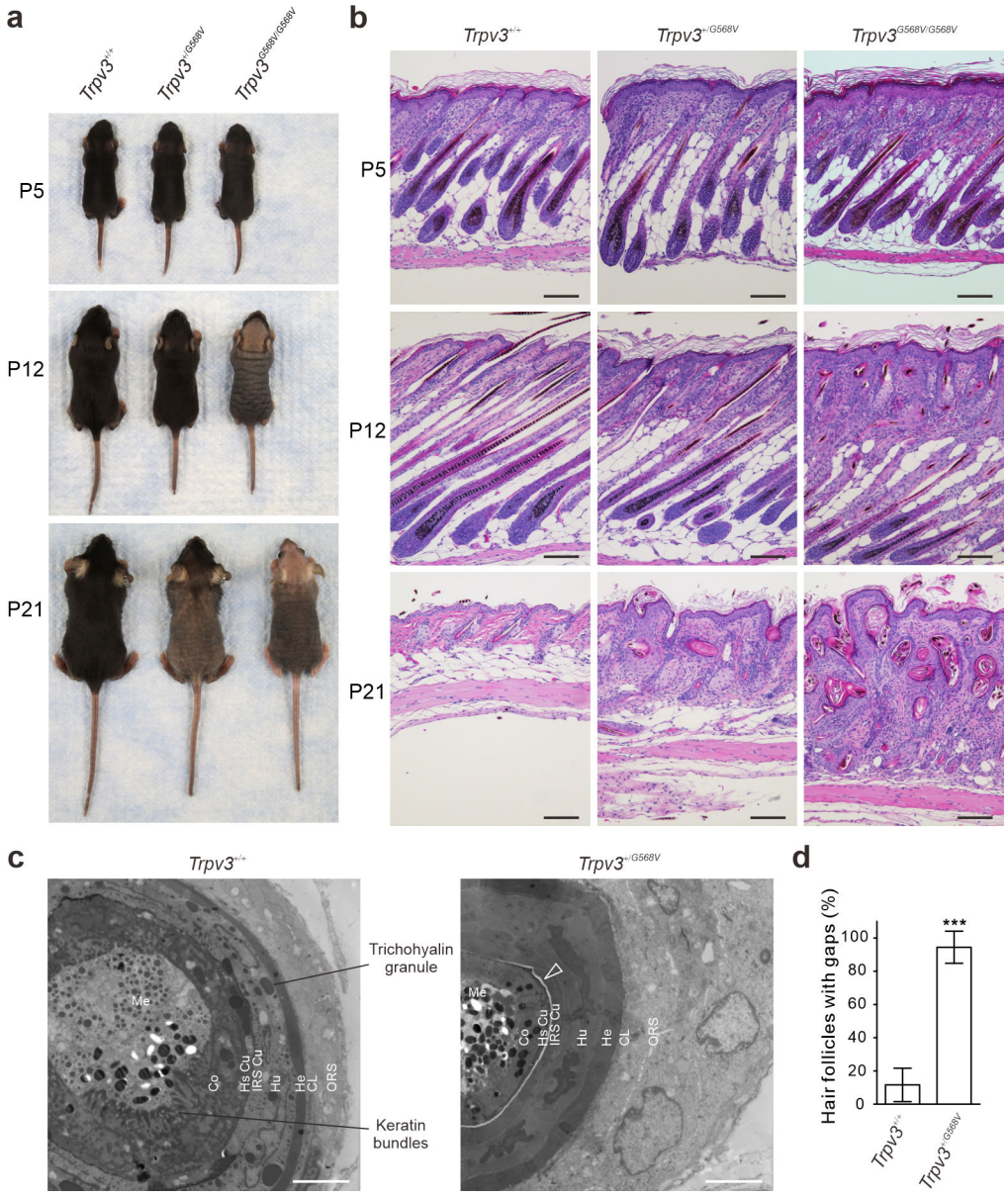

Figure 2. Hair phenotype in *Trpv3* knock-in mouse model.

(**a - b**) Appearance (**a**) and histology (**b**) of dorsal skins from *Trpv3*$^{+/+}$, *Trpv3*$^{+/G568V}$ and *Trpv3*$^{G568V/G568V}$ littermates. (**c**) Transmission electron microscopy of hair follicles at approximately 500 μm depth. Arrow points to the electron-light gap between the IRS and HS Cu. ORS, outer root sheath; CL, companion layer; He, Henle's layer; Hu, Huxley's layer; IRS Cu, inner root sheath cuticle; HS Cu, hair shaft cuticle; Co, cortex; Me, medulla. (**d**) Quantification of the gap between the IRS and HS Cu in (**c**). n = 3 mice per genotype. ≥ 18 hair follicles were examined per genotype. Data are presented as mean ± SD. *** P < 0.001 (Two-tailed Student's unpaired *t* test). Scale bar = 100 μm (**b**), 4 μm (**c**).

Author Manuscript Author Manuscript Author Manuscript Author Manuscript

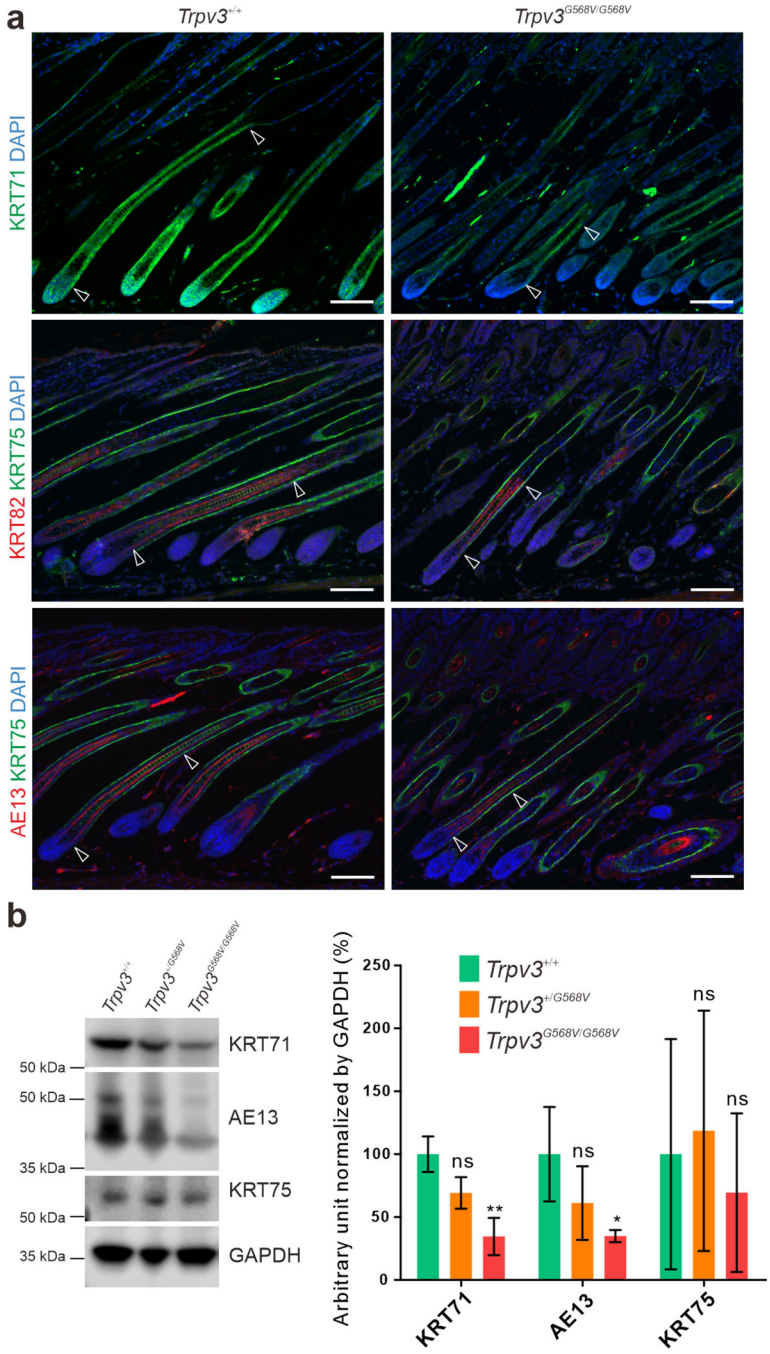

Figure 3. Impaired hair follicle differentiation in *Trpv3* knock-in mice.

(**a**) Immunofluorescence labeling of KRT71 (green), KRT75 (green), KRT82 (red), and hair cortex keratins detected by the AE13 antibody (red) in dorsal skins of P12 *Trpv3*$^{+/+}$ and *Trpv3*$^{G568V/G568V}$ littermates. Arrow heads point to the portions of hair follicles positive for KRT71, KRT82, and AE13, respectively. Nuclei were stained with DAPI (blue). (**b**) Western blotting of KRT71, hair cortex keratins (AE13), and KRT75, and quantifications. Whole length images can be found in Supplementary Figure S6. n = 3 mice per genotype. Data are

Author Manuscript Author Manuscript Author Manuscript Author Manuscript

presented as mean ± SD. * $P < 0.05$. ** $P < 0.005$. ns, not significant. One-way ANOVA analysis was followed by Dunnett's Multiple Comparison Test. Scale bar = 100 μm (**a**).

Author Manuscript Author Manuscript Author Manuscript Author Manuscript

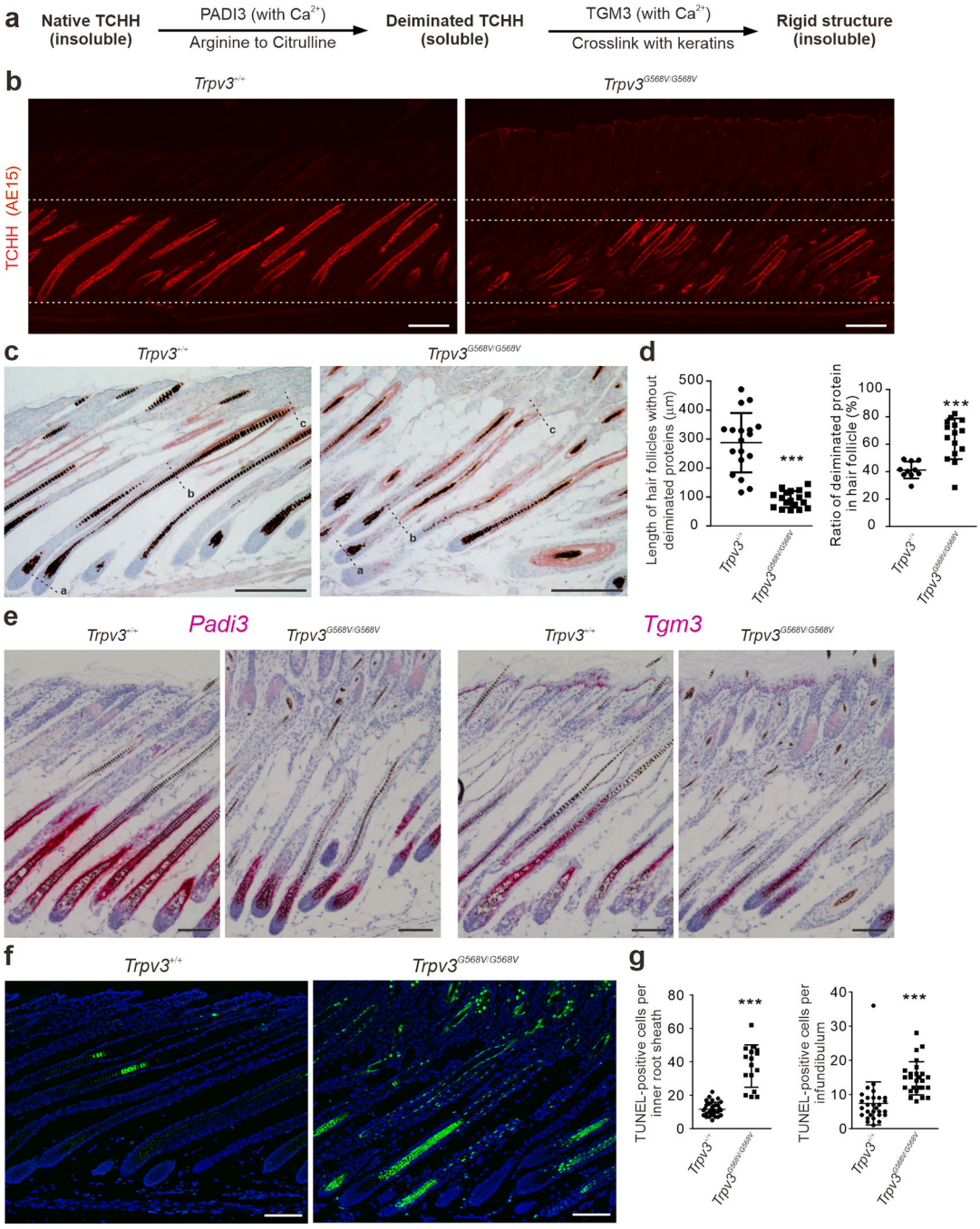

Figure 4. Late differentiation of dorsal hair follicles in P12 *Trpv3* knock-in mice.

(**a**) Illustration of posttranslational modification of TCHH. (**b - c**) Immunofluorescence labeling of TCHH (red, **b**) and immunohistochemistry of deiminated proteins (ruby red, **c**). (**d**) Quantification of distance between the Auber's line (point a) and the most proximal signal of deiminated proteins (point b), and ratio of deiminated proteins (point b to c) and nonpermanent portion of the hair follicles (point a to c), as shown in (**c**). n = 3 mice per genotype. ≥ 10 hair follicles per genotype were examined. Data are presented as mean ± SD. *** P < 0.001 (Two-tailed Student's unpaired *t* test). (**e**) *In situ* hybridization of *Padi3* (pink,

Author Manuscript Author Manuscript Author Manuscript Author Manuscript

left) and *Tgm3* (pink, right). (**f - g**) TUNEL staining and quantification. n = 5 mice per genotype and ≥ 16 hair follicles per genotype were examined. Data are presented as mean ± SD. *** P < 0.001 (Two-tailed Student's unpaired *t* test). Scale bar = 200 μm (**b - c**), 100 μm (**e - f**).

Author Manuscript Author Manuscript Author Manuscript Author Manuscript

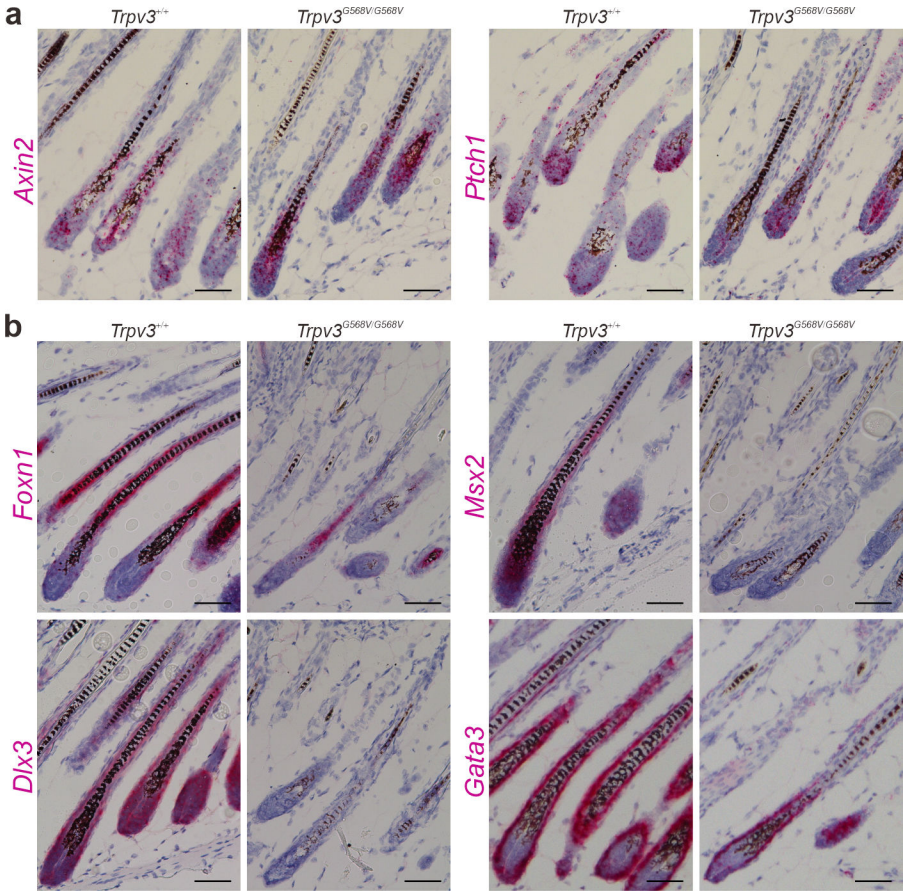

Figure 5. Examination of regulators for hair follicle induction and differentiation.

(**a - b**) *In situ* hybridization of *Axin2* (pink, left) and Ptch1 (pink, right) in (**a**), and *Foxn1* (pink, top left), *Msx2* (pink, top right), *Dlx3* (pink, bottom left) and *Gata3* (pink, bottom right) in (**b**), in dorsal skins of P12 *Trpv3*$^{+/+}$ and *Trpv3*$^{G568V/G568V}$ littermates. For (**a - b**), nuclei were stained with hematoxylin (blue). Scale bar = 50 μm (**a - b**).

Author Manuscript Author Manuscript Author Manuscript Author Manuscript

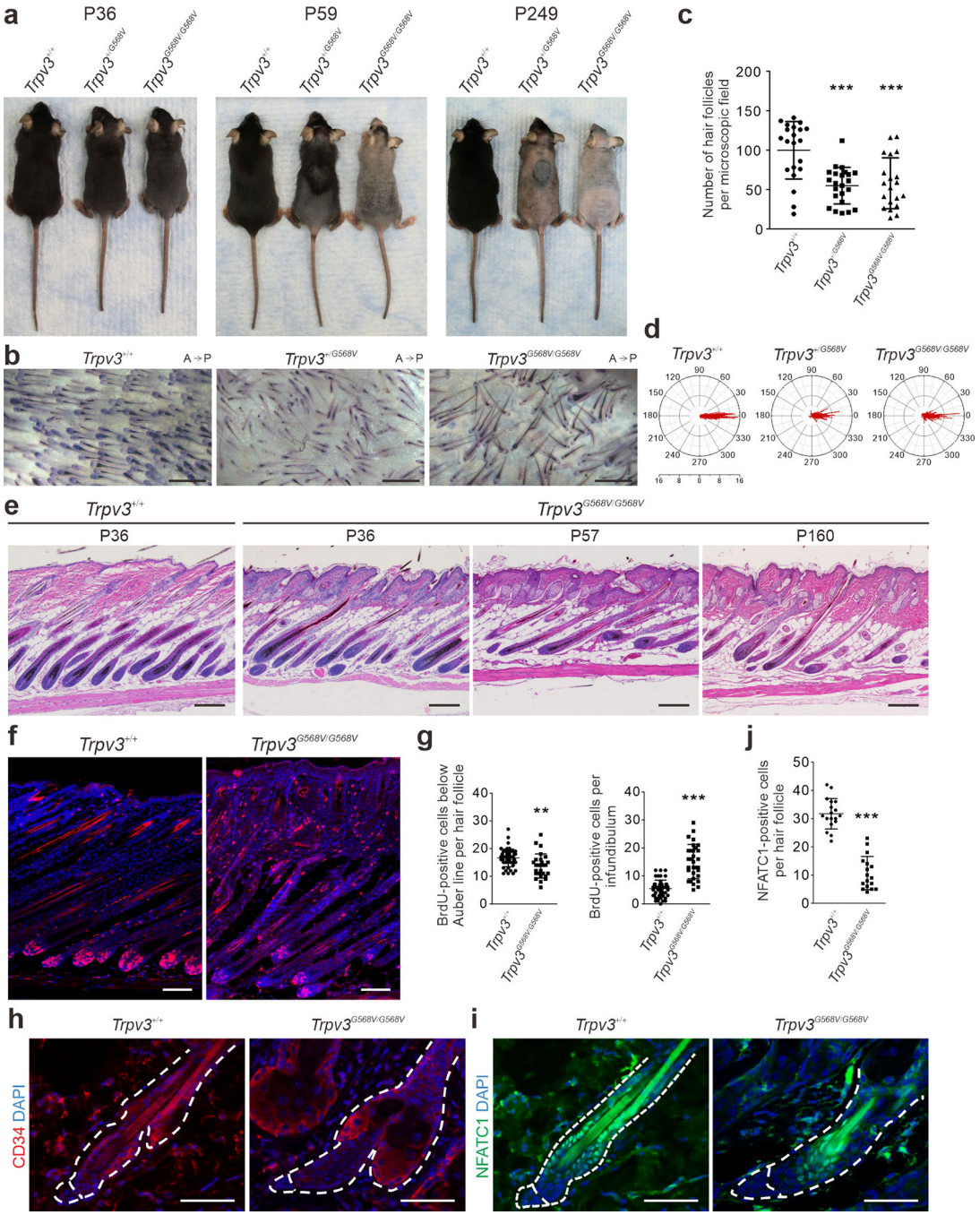

Figure 6. Impaired hair regeneration in *Trpv3* knock-in mice.

(**a**) Appearance at indicated age. (**b - d**) Alkaline phosphatase staining of dorsal skins of P249 littermates (**b**), and quantification of hair follicle density (**c**) and anterioposterior orientation (**d**). A, anterior. P, posterior. Radial axis represents the number of hair follicle in that specific angle. n = 4 mice per genotype and ≥ 20 microscopic fields per genotype were examined. Number of hair follicles evaluated: $Trpv3^{+/+}$, 278; $Trpv3^{+/G568V}$, 262; $Trpv3^{G568V/G568V}$, 283. Data are presented as mean ± SD. *** P < 0.001 (One-way ANOVA analysis was followed by Dunnett's Multiple Comparison Test). (**e**) Histology of dorsal skins

Author Manuscript Author Manuscript Author Manuscript Author Manuscript

at indicated postnatal days. (**f - g**) BrdU labeling and quantification in P12 littermates. n = 5 mice per genotype and ≥ 27 hair follicles per genotype were examined. Data are presented as mean ± SD. *** P < 0.001, ** P < 0.05 (Two-tailed Student's unpaired *t* test). (**h - j**) Immunofluorescence labeling of CD34 (**h**) and NFATC1 (**i**), and quantification (**j**) in P48 littermates. n = 3 mice per genotype and ≥ 17 hair follicles per genotype were examined. Data are presented as mean ± SD. *** P < 0.001 (Two-tailed Student's unpaired *t* test). Scale bar = 500 μm (**b**), 200 μm (**e**), 100 μm (**f**), 50 μm (**h - i**).